Nickel(II) Complexes Incorporating Pyridyl, Imine and Amino Chelate Ligands: Synthesis, Structure, Isomer Preference, Structural Transformation and Reactivity Towards Nickel(III) Derivatives

Suparna Banerjee,[a] Jaydip Gangopadhyay,[b] Can-Zhong Lu,[c] Jiu-Tong Chen,[c] and Ashutosh Ghosh*[a]

Keywords: Coordination modes / Isomer specificity / N ligands / Nickel / Structural transformation

Facile condensation of 2-acetylpyridine with ethylenediamine in a 1:1 or 2:1 molar ratio yielded two neutral ligands with different denticity: 1-amino-4-(2-pyridyl)-3-azapent-3-ene (tridentate, L^1) and 2,7-bis(2-pyridyl)-3,6-diazaocta-2,6-diene (tetradentate, L^3), respectively. Replacing the ketone with 2-pyridinecarboxaldehyde gave a similar set of condensates (L^2 and L^4). The tridentate mono-Schiff bases (L^1 and L^2) react smoothly with $Ni(ClO_4)_2{\cdot}6H_2O$ furnishing the brown bis-chelate complexes (**1a** and **1b**) with an NiN_6 coordination sphere, while the tetradentate bis-Schiff bases (L^3 and L^4) form green pseudo-octahedral complexes (**2a** and **2b**) in which Ni^{II} is present in an N_4O_2 coordination environment. The isomer specificity for both types of complexes is conspicuous from the representative X-ray structures of **1a** and **2a**. *cis-trans-cis* and *cis-cis-trans* isomers are found exclusively for **1** and **2**, respectively. The crystal structure of **2a** reveals O–H···O hydrogen bond interactions assembling alternating cations and anions in an infinite chain-like array. Cyclic voltammetric measurements of **1** and **2** in MeCN solution show a quasi-reversible one-electron oxidation near 0.95 and 0.87 V (vs. SCE), respectively, attributed to a Ni^{III}-Ni^{II} redox couple. Another irreversible Ni^{IV}-Ni^{III} redox response was observed at higher potential near 1.70 and 1.80 V (vs. SCE) for **1** and **2**, respectively. Complexes **1** and **2** display a weak, broad d-d transition band along with a charge-transfer transition. Magnetic susceptibility measurements (at 298 K) confirmed that the spin states of the Ni^{II} centres in **1** and **2** are same, $S = 1$, in agreement with an octahedral configuration. Complexes **1** form stable reddish-brown Ni^{III} complexes (**3**) under exhaustive constant-potential electrolysis treatment. The Ni^{III} complexes display axial EPR spectra both at 298 K and 77 K with $g_\perp > g_\parallel$ indicating the presence of an unpaired electron primarily on the metal centre. Complexes of type **1** and **3** exhibit virtually superimposable cyclic voltammograms in a reverse electrode scan study which confirms no change in the coordination sphere on going from **1** to **3**. The effective magnetic moment values (ca. 2.10 μ_B) of **3** suggest a significant orbital contribution to the paramagnetism, consistent with a tetragonally distorted low spin $3d^7$ system. A colour change phenomenon has been observed for type **2** complexes.

Introduction

Over the last few decades considerable attention has been paid to rationalizing the underlying chemical aspects regarding the stabilizing and destabilizing factors of Ni^{III} species derived from Ni^{II} precursors in various coordination environments.[1,2]

We report here the synthesis and structural features of new NiN_6 and NiN_4O_2 coordination spheres derived from neutral mono-Schiff bases and bis-Schiff bases respectively, as ligands. The electrochemical behaviour of all the members of the two families was investigated with the aim of determining the relative stability of progressively higher oxidation states (+II, +III and +IV) and possible transformations thereof.[2–4] The NiN_6 complexes smoothly undergo electrochemical one-electron oxidation at ambient temperature to give Ni^{III} complexes with identical coordination environments. Hence this type of bis-chelate complex can be modelled to trigger the reversible electron-transfer reactions that are essential for biological[5] as well as catalytic[6] processes. The molecular packing of a representative of the NiN_4O_2 family (**2a**) has revealed two sterically uncongested ONN triangular faces forming O···O hydrogen-bond interactions with counter perchlorate anions. Under the appropriate conditions these open faces can be utilised to accommodate small guest molecules, an area that has been much less explored than the more common crown ethers,[7] imine

[a] Department of Chemistry, University College of Science and Technology, University of Calcutta,
92, A.P. C. Road, Kolkata 700 009, India
[b] Department of Inorganic Chemistry, Indian Association for the Cultivation of Science,
Kolkata 700 032, India
[c] The State Key Laboratory of Structural Chemistry, Fujian Institute of Research on the Structure of Matter, The Chinese Academy of Sciences,
Fuzhou, Fujian 350002, P. R. China

Schiff-base macrocycles[8] and cryptands.[9] A thermogravimetric experiment followed by spectroscopic characterisation showed a change from a six-coordinate octahedral geometry to a four-coordinate distorted square planar form by releasing two *trans* water co-ligands. The observed colour change (green→ red) is associated with this structural change, as is common for other Ni^{II} complexes in different coordination environments.[10]

Results and Discussion

Synthesis of the Complexes

The tridentate and tetradentate Schiff bases 1-amino-4-(2-pyridyl)-3-azapent-3-ene and 2,7-bis(2-pyridyl)-3,6-diazaocta-2,6-diene (general abbreviation, L) have been employed as chelating ligand in the present work. The analogous 2-pyridylcarboxaldimine ligands have also been used for a comparative study. The four complexes reported in this context belong to two different types **1** and **2**.

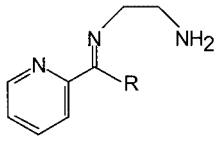

L^1 (R = CH_3)

L^2 (R = H)

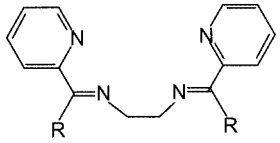

L^3 (R = CH_3)

L^4 (R = H)

The brown bis-chelate complexes **1** are formed in excellent yield upon reacting $Ni(ClO_4)_2{\cdot}6H_2O$ with L^1 or L^2 in a 1:2.2 molar ratio in aqueous methanol under reflux (Scheme 1).

$Ni(ClO_4)_2{\cdot}6H_2O$ reacts smoothly with either L^3 or L^4 in a 1:1.2 molar ratio in aqueous methanol under reflux to give the green complexes **2** in high yield (Scheme 2). Complexes **2** undergo an interesting dehydration-rehydration process, which is influenced by temperature and pressure. At ambient temperature and normal pressure the complexes are stable; the effect of heating on the dehydration process will be examined later.

Attempts to perform a template synthesis by condensation of the appropriate aldehyde or ketone with ethylenediamine followed by complexation with the metal ion in situ, maintaining the 2:2:1 and 2:1:1 molar ratio necessary for the formation of complexes **1** and **2** gave the exclusive formation of **1** due to the chelate effect.

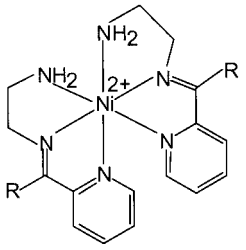

1a (R = CH_3)

1 (R = H)

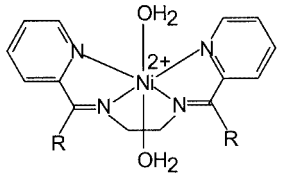

2a (R = CH_3)

2b (R = H)

The perchlorate salts act as 1:2 electrolytes in acetonitrile solution (Λ = 245−255 $\Omega^{-1}{\cdot}cm^2{\cdot}mol^{-1}$). Complexes of type **1** give the stable oxidised derivatives **3** under constant electrolysis treatment, whereas type **2** complexes are inherently unstable towards electrolytic treatment.

The *cis-trans-cis* and *cis-cis-trans* disposition of the N^pN^p-N^iN^i-N^aN^a (in type **1** complexes) and N^pN^p-N^aN^a-O^wO^w (in type **2** complexes) donor sets (N^p is pyridyl nitrogen, N^i is imine nitrogen, N^a is amino nitrogen and O^w is oxygen of water) are the striking features of these complexes.

Geometrical Preference and Structural Features

[Ni(L^1)$_2$](ClO$_4$)$_2$

This complex has a distorted octahedral geometry. The ligand encapsulates the divalent metal ion through six ligating nitrogen atoms from two pyridyl [N(1) and N(4)], two imine [N(2) and N(5)] and two amino [N(3) and N(6)] groups (Figure 1, Table 1). Several isomers are theoretically possible considering the relative arrangement of three types of coordinated nitrogen atoms around the metal centre, although the only one encountered here has the pyridine ni-

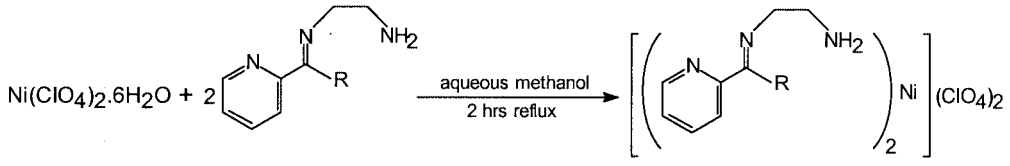

Scheme 1

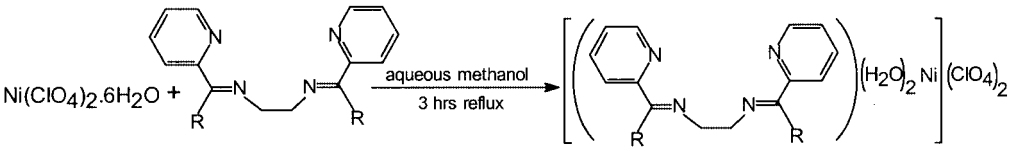

Scheme 2

trogen atoms in the *cis* position and the imine nitrogen atoms in the *trans* positions, thereby leaving two *cis* positions available for the amino nitrogen donors. The *trans* disposition of two N^i donor sites in a *cis-trans-cis* geometry ensures competition between them for the same metal d-orbital, thus minimising the back-bonding stabilisation. This *cis-trans-cis* geometry (no NiN^i interaction) is sterically more favourable than any of the possible unobserved isomers (*cis-cis-trans, trans-cis-cis*) having a *cis* NiN^iN^i orientation (two NiN^i interactions). Evidently the steric relaxation completely offsets the back-bonding disadvantage in the case of the *cis-trans-cis* isomer and none of the other isomers are observed.

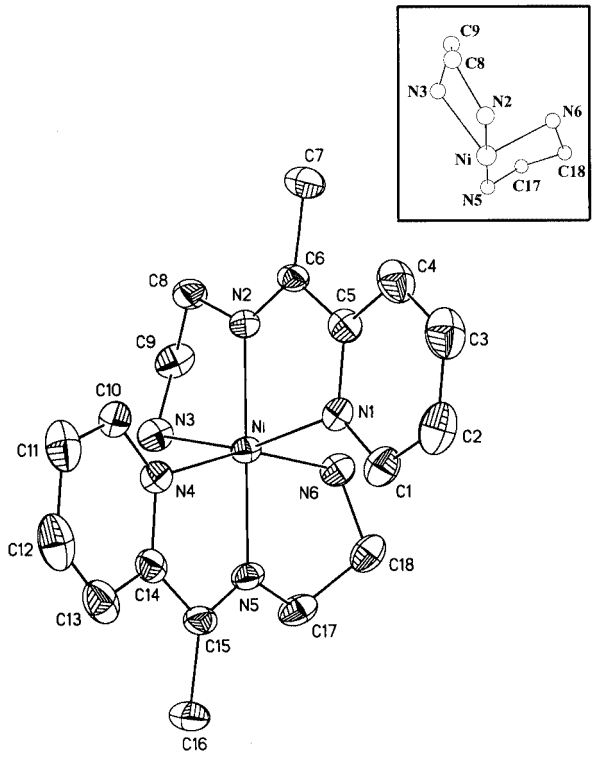

Figure 1. A perspective view and atom-labelling scheme of the complex cation of $[Ni(L^1)_2](ClO_4)_2$ (**1a**); all non-hydrogen atoms are represented by their 25% thermal probability ellipsoids; the inset shows the conformations of the dimethylene-bridged chelate rings

Table 1. Selected bond lengths (Å) and angles (°) for $[Ni(L^1)_2](ClO_4)_2$

Ni−N5	2.008(5)	Ni−N2	2.013(5)
Ni−N6	2.119(5)	Ni−N4	2.120(7)
Ni−N1	2.123(5)	Ni−N3	2.143(6)
N5−Ni−N2	179.4(2)	N5−Ni−N6	81.9(2)
N2−Ni−N6	97.5(2)	N5−Ni−N4	77.5(2)
N2−Ni−N4	103.1(2)	N6−Ni−N4	158.6(2)
N5−Ni−N1	102.5(2)	N2−Ni−N1	77.8(2)
N6−Ni−N1	91.7(2)	N4−Ni−N1	87.3(2)
N5−Ni−N3	99.0(2)	N2−Ni−N3	80.7(2)
N6−Ni−N3	94.4(3)	N4−Ni−N3	94.3(2)
N1−Ni−N3	158.2(2)		

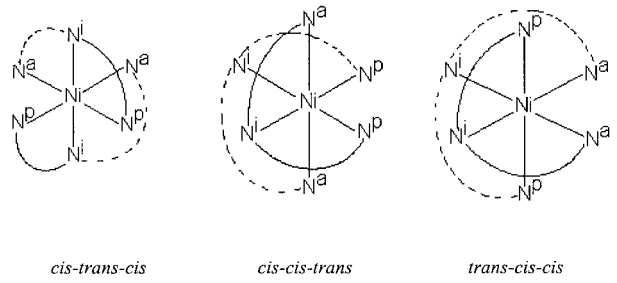

The N(1), N(3), N(4) and N(6) atoms define a severely distorted basal plane (mean deviation 0.39 Å). The five-membered chelate rings [Ni, N(1), C(5), C(6) and N(2)] and [Ni, N(4), C(14), C(15), and N(5)] along with the conjugated pyridyl moieties constitute satisfactory planes (mean deviation 0.06 Å and 0.07 Å respectively). The two remaining saturated five-membered metallo rings are out of plane (average mean deviation 0.16 Å) and the dimethylene bridges assume a twisted skew conformation (see inset, Figure 1). As a whole, two $Ni(L^1)$ fragments are not planar (average mean deviation 0.11 Å) essentially due to steric repulsion between the two dimethylene-bridged chelate rings. Two pyridylimine metallo rings enjoy extended π-electron delocalisation, inducing a more rigid nature and a decrease in the chelate bite angles (average 77.7°). On the contrary, the twisted dimethylene-bridged metallo rings are flexible with larger (closer to 90°) bite angles (average 81.3°). All metal-nitrogen bond lengths are consistent with literature values.[1,11−14] The $Ni-N^i$ bonds are shorter than the $Ni-N^p$ and $Ni-N^a$ bonds by about 0.11 Å. This $Ni-N^i$ bond-shortening stems from the better π-accepting ability of imine (C=N) functions than the N^p and N^a coordination sites.

[Ni(L³)(H₂O)₂] (ClO₄)₂

The *cis-cis-trans* geometry with respect to N^p, N^i and O^w donor sites is found exclusively rather than another possible *trans-cis-cis* isomer for complexes **2**. This isomer specificity primarily stems from the better degree of $Ni-N^i$ back-bonding in the *cis-cis-trans* isomer due mainly to the presence of a stronger *trans* σ-donor N^p atom (in the *trans-cis-cis* geometry a weaker O^w atom is *trans* to the $Ni-N^i$ bond) sharing the same metal d-orbital. Moreover the *cis-cis-trans* orientation (devoid of NiO^w interactions) is better in a steric sense than the unprecedented *trans-cis-cis* isomer with a *cis*-NiO^wO^w disposition (two destabilising NiO^w interactions). Therefore, we can rationalize the exclusive occurrence of the *cis-cis-trans* isomer in terms of both electronic and steric factors.

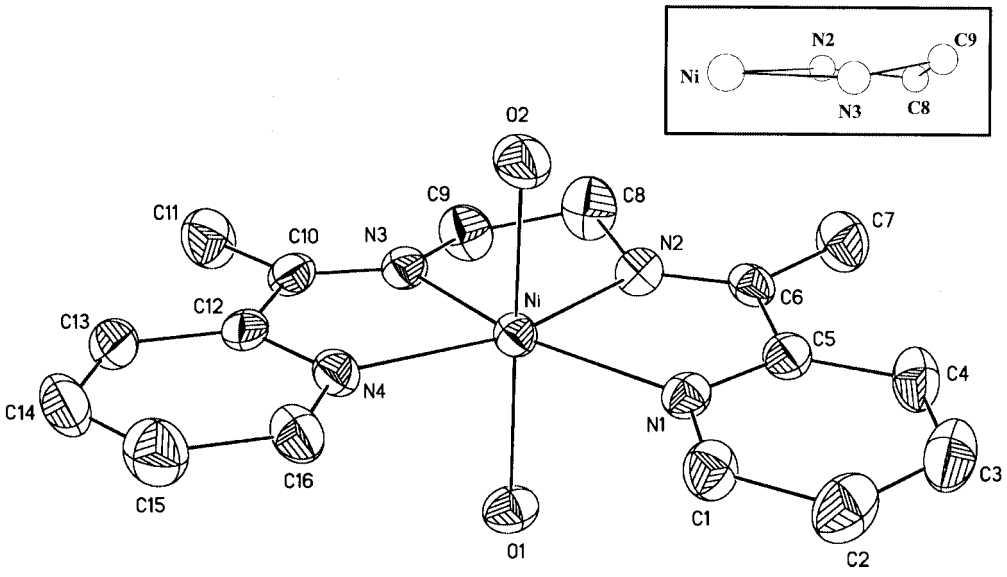

Figure 2. A perspective view and atom-labelling scheme of the complex cation of $[Ni(L^3)(H_2O)_2](ClO_4)_2$ (**2a**); all non-hydrogen atoms are represented by their 25% thermal probability ellipsoids; the inset shows the conformation of the dimethylene-bridged metallo ring

A molecular view of **2a** is presented in Figure 2, and selected bond parameters are listed in Table 2. The Ni^{II} ion sits in a reasonably planar equatorial plane (mean deviation 0.04 Å) defined by the N(1), N(2), N(3) and N(4) atoms.

Table 2. Selected bond lengths (Å) and angles (°) for $[Ni(L^3)(H_2O)_2](ClO_4)_2$

Ni−N2	1.997(6)	Ni−N3	2.002(6)
Ni−N4	2.071(6)	Ni−N1	2.088(6)
Ni−O2	2.100(6)	Ni−O1	2.118(5)
N2−Ni−N3	82.8(2)	N2−Ni−N4	161.5(3)
N3−Ni−N4	78.9(3)	N2−Ni−N1	78.5(2)
N3−Ni−N1	161.2(2)	N4−Ni−N1	119.9(2)
N2−Ni−O2	91.5(3)	N3−Ni−O2	95.0(2)
N4−Ni−O2	87.3(2)	N1−Ni−O2	88.0(2)
N2−Ni−O1	94.4(3)	N3−Ni−O1	92.4(2)
N4−Ni−O1	89.2(2)	N1−Ni−O1	86.6(2)
O2−Ni−O1	171.1(3)		

Hard donors, like oxygen atoms, coordinated along the axial direction force the metal ion to sit in the basal plane. Individual π-conjugated chelate rings are essentially completely planar (mean deviation 0.01 Å in both cases). The dimethylene-bridged chelate ring [Ni, N(2), C(8), C(9), N(3)] is only approximately planar (mean deviation 0.08 Å) as compared to the π-conjugated chelate fragments. The overall planarity of the $Ni(L^3)$ motif (mean deviation 0.08 Å) is disturbed because of the twisted dimethylene bridging segment (see inset, Figure 2). The chelate bite angles of N(4)−Ni−N(3) and N(1)−Ni−N(2) are 78.9(3) and 78.5(2)°, respectively, and are less than that observed for N(2)−Ni−N(3) [82.8(2)°]. Like **1a**, the difference in bite angles (>4°) is fully consistent with the varying degree of flexibility of the chelate rings. A comparison between the $Ni-N^p$ and $Ni-N^i$ distances clearly reveals a bond shortening of about 0.08 Å (on average) for the latter $Ni-N^i$ type, attributable to additional d(metal) → π*(C=N) back-bonding. Indeed this dative back-bonding is facilitated in presence of the *trans* N^p atom (strong σ-donor) sharing the same d orbital of the metal as the N^i donor. The average $Ni-N^p$ distance in **2a** is appreciably shorter (ca. 0.04 Å) than that observed for **1a**. The underlying reason presumably arises from the different relative orientations of the N^p and N^i donor atoms around the metal centres (*cis* for **2a** and *trans* for **1a**), inducing the pyridyl moiety to act as a better σ-donor in **2a**. The $Ni-O^w$ bonds are relatively weak[15,16] compared to other aquated Ni^{II} systems. The presence of intermolecular hydrogen-bonding accounts for the lengthening of the $Ni-O^w$ bonds, and is primarily an electronic effect. The effect of this unsymmetrical hydrogen bonding through two-coordinated water molecules is reflected in a bending of the O^w-Ni-O^w axis, making an angle of 171.1(3)°.

The uncoordinated perchlorate ions of **2a** form a hydrogen-bonded network with the two axially coordinated water molecules of the cationic part of the complex. Two water molecules of the Ni^{II} complex cation are engaged in three unsymmetrical O···O hydrogen-bond contacts with two open ONN triangular faces (average surface area, ≈4.1 $Å^2$) avoiding unwanted steric interactions. The molecular packing diagram reveals that the coordinated water molecules of a cation form hydrogen bonds with perchlorate ions belonging to two different asymmetric units. The relevant O···O contacts [O(1E)···O(8A): 2.850(6) Å, O(2E)···O(3C): 2.876(8) Å and O(2E)···O(10E): 2.722(8) Å] generate a chain-like cationic assembly in which alternating cations lie in an almost parallel fashion, as illustrated in Figure 3.

Electronic Spectra

The electronic spectra of the four complexes **1a**, **1b**, **2a** and **2b** were recorded both in the solid state (nujol mull)

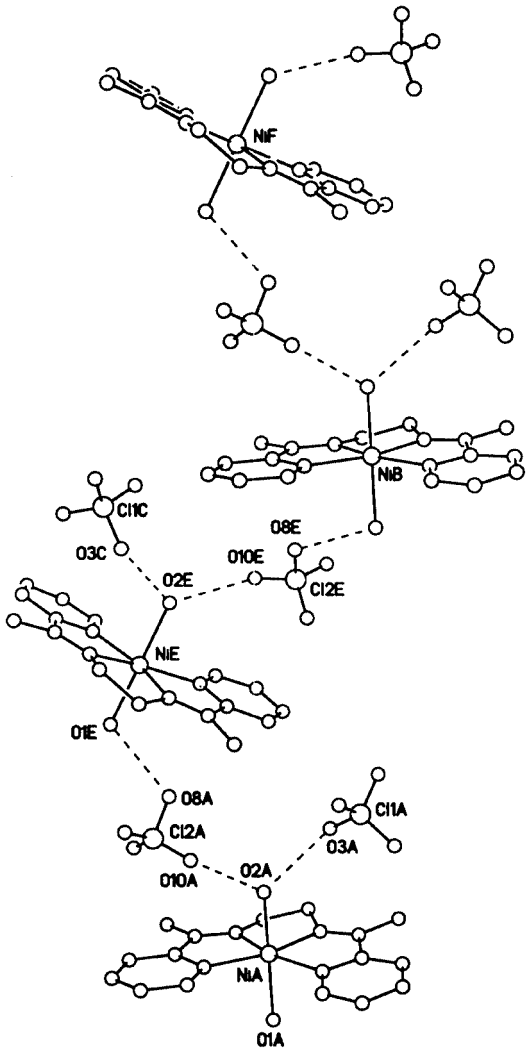

Figure 3. Molecular packing view of **2a** along the *x*-direction

and in acetonitrile solution. No significant differences were observed. A broad band is observed near 800 nm, well separated from the second transition at about 510 nm for both **1** and **2**. The third d-d band appears near 350 nm and is partly obscured by a strong charge-transfer transition. The three absorption peaks are assigned to transitions from the $^3A_{2g}$ ground state to $^3T_{2g}$, $^3T_{1g}(F)$ and $^3T_{1g}(P)$ excited states. In addition, a weak peak appears near 750 nm for complexes **2**, interpretable on the basis of a spin-forbidden $^3A_{2g} \rightarrow {}^1E_g$ transition. The calculated values of *Dq* lie in the range 1250−1260 cm^{-1} for all complexes, and are in agreement with literature values.[17,18] The reddish-brown Ni^{III} complexes **3** are characterised by an LMCT transition at about 425 nm with a shoulder near 645 nm.

Electrochemistry

With the aim of investigating the extent of stabilisation of nickel(II) species towards both oxidation and reduction, and thereby the possibility of accessing of variable valence states, cyclic voltammetry experiments were performed on **1** and **2** (Table 3).

Table 3. Electrochemical data for all divalent nickel complexes

Compound	$E_{1/2}$/V (ΔE_p/mV)[a]	
	Ni^{III}-Ni^{II} couple	Ni^{IV}-Ni^{III} couple
1a	0.95 (110)	1.69
1b	0.96 (110)	1.72
2a	0.85 (100)	1.78
2b	0.87 (100)	1.80

[a] ΔE_p = Peak-to-peak separation.

$[Ni(L^1)_2](ClO_4)_2$ and $[Ni(L^2)_2](ClO_4)_2$ are electroactive in acetonitrile solution (TEAP as supporting electrolyte) displaying two one-electron cyclic voltammetric responses with $E_{1/2}$ near +0.95 and +1.70 V vs. the saturated calomel electrode (SCE). Type **1** complexes undergo chemically reversible ($i_{pa}/i_{pc} \approx 1$) and electrochemically quasi-reversible (ΔE_p = 110 mV) one-electron oxidative responses due to the $[Ni^{III}(L^{1/2})_2]^{3+}/[Ni^{II}(L^{1/2})_2]^{2+}$ couple, near 0.95 V as observed for bis-pyridylazonaphthol-chelated complexes of Ni^{II}.[19] Appreciable reversibility is also inferred from the i_{pa},i_{pc} vs. $\nu^{1/2}$ plot, which is nearly constant for different scan rates (0.025, 0.05, 0.075 and 0.1 V/sec). The irreversible redox signal encountered near +1.70 V is attributed to the $Ni^{4+/3+}$ response. No voltammetric response consistent with a $Ni^{2+/1+}$ reduction is observed. Further, absence of a $Ni^0(s) \rightarrow Ni^{2+}$ stripping peak emphasises the reluctance of $[Ni^{II}(L^{1/2})_2]^{2+}$ to undergo a two-electron reduction. The relevant electron-transfer processes correlating metal valence span from +2 to +4 can be represented by Equation (1).

$$[Ni^{IV}(L^{1/2})_2]^{4+} \underset{-e^-}{\overset{+e^-}{\rightleftharpoons}} [Ni^{III}(L^{1/2})_2]^{3+} \underset{-e^-}{\overset{+e^-}{\rightleftharpoons}} [Ni^{II}(L^{1/2})_2]^{2+} \quad (1)$$

Such a relatively high $E_{1/2}$ value for the $Ni^{3+/2+}$ redox transformation is typical in complexes where nickel is in a mixed sulfur-nitrogen coordination environment.[20] Even higher $E_{1/2}$ values (ca. 1.6 V) have been reported for the $[Ni(bipy)_3]^{3+}/[Ni(bipy)_3]^{2+}$ couple.[21] The absence of any satellite response is fully consistent with the exclusive occurrence of one isomer (*cis-trans-cis*), in solution.

The redox behaviours of $[Ni(L^3)(H_2O)_2]$ $(ClO_4)_2$ and $[Ni(L^4)(H_2O)_2]$ $(ClO_4)_2$ follow a similar trend as **1a** and **1b**. Complex **2** in acetonitrile exhibits a quasi-reversible (ΔE_p = 100 mV) one-electron oxidation near 0.87 V consistent with the $[Ni^{III}(L^{3/4})(H_2O)_2]^{3+}/[Ni^{II}(L^{3/4})(H_2O)_2]^{2+}$ couple. The observed shift (in 0.08 V) of the $E_{1/2}$ value toward negative potential compared to the $E_{1/2}$ observed for $[Ni(L^{1/2})_2]^{3+/2+}$ accentuates the relative stabilisation of the Ni^{III} species derived from type **2** complexes. The *trans* disposition of the two imine donor motifs in $[Ni(L^{1/2})_2]^{2+}$ which becomes a *cis* orientation for $[Ni(L^{3/4})(H_2O)_2]^{2+}$ obviously facilitates greater delocalisation of the metal electron density, resulting in a higher potential barrier for the formation of Ni^{III} species from the latter complexes. This was observed experimentally from the irreversible peak near +1.80 V, ascribed to a

$Ni^{4+/3+}$ redox process. This oxidative response is shifted to positive potential by 0.10 V in comparison with the $Ni^{4+/3+}$ couple for **1**. Like **1**, no $[Ni^{II}(L^{3/4})(H_2O)_2]^{2+}/[Ni^{I}(L^{3/4})(H_2O)_2]^{1+}$ redox couple is observed in acetonitrile solution.

In order to exclude any possibility of rapid isomerisation, cyclic voltammograms of **1** and **2** were run at various temperatures. Strong $Ni^{3+/2+}$ and $Ni^{4+/3+}$ responses for **1** and **2** were observed at 288 and 308 K at very nearly the same formal potential, and with similar current heights, as observed for the cyclic voltammograms recorded at 298 K (discussed earlier). Therefore, in this context the temperature effect upon the redox couples is not significant.

IR Spectra and Magnetism

The two primary NH_2 stretching modes are seen in type **1** complexes near 3340 and 3290 cm^{-1} as sharp bands (doublet) for the asymmetric and symmetric vibrations, respectively. The imine (C=N) stretch appears at about 1660 cm^{-1}, and the red shift of this C=N absorption of about 20 cm^{-1} on going from the free ligands (L^1, L^2) to the complexes indicates the weak π-accepting behaviour of the chelated ligands. The type **2** complexes exhibit a broad band in the range 3410−3440 cm^{-1}, assigned to the antisymmetric and symmetric O−H stretching vibrations of coordinated water molecules. ν_{Ni-O} appears near 450 cm^{-1} for **2**.[22] The diagnostic C=N stretch is observed near 1650 cm^{-1}, and is shifted to lower frequency by about 30 cm^{-1} relative to the free ligands. The difference in imine stretching frequencies of complexes **1** and **2** confirms the greater electron-withdrawing effect of the chelating bis-Schiff bases (L^3, L^4) in the latter. Broad structured ν_3 and sharp ν_4 vibrations of the perchlorate counteranion are observed near 1100 and 630 cm^{-1} for **1** and **2**, respectively.

The effective magnetic moment data of complexes **1** and **2** (polycrystalline state) clearly confirm the presence of two unpaired electrons ($t_2^6e^2$) in a pseudo-octahedral environment, in agreement with a high-spin configuration ($S = 1$). The magnetic moment values of 3.12, 3.15, 3.06 and 3.05μ_B at 298 K for **1a**, **1b**, **2a** and **2b**, respectively, suggest an appreciable orbital contribution to the spin-only moments.[23]

NMR Spectra

The ^1H NMR spectra of **1** (bulk material, in $[D_6]$DMSO) display paramagnetically shifted resolved signals of the aromatic, aliphatic and amino protons. The pyridyl and methylene proton resonances occur in the ranges $\delta = 6-12$ and $-12-45$ ppm, respectively. The methyl (**1a**) and aldimine (**1b**) hydrogen atom signals appear as singlets in the region $\delta = 2.5-3.5$ and 8−10 ppm, respectively. The amino protons resonate at lower field in the region $\delta = 75-95$ ppm. The absence of satellite peaks clearly confirms the exclusive occurrence of one isomer. The distinct spin-spin structures of the corresponding signals remove any scope for a rapid equilibrium between the possible isomers in solution. These results mean that the stereochemistry of **1** in the solid state is also retained in solution and no interconversion takes place as this would otherwise result in an averaging of nonequivalent protons.

Similarly in **2**, the pyridyl and methylene proton signals appear in the region $\delta = 7-14$ and $-7-30$ ppm respectively. The methyl (**2a**) and aldimine (**2b**) hydrogen resonances occur in similar regions to those of **1**. The aqua hydrogen resonances fall in the range $\delta = 60-85$ ppm. The large range of the NMR signals of **2** is consistent with its paramagnetic nature.

Thermal Analysis and Structural Transformation

Complexes **2a** and **2b** are both green and possess an octahedral geometry with axially coordinated water molecules. The TG curve reveals that upon heating both **2a** and **2b** undergo dehydration in the temperature range 50−95 °C and 60−100 °C, respectively, corresponding to the weight loss of two water molecules (observed: 6.96 and 7.01%; calculated: 6.43 and 6.77% for **2a** and **2b**, respectively). The anhydrous compounds begin to decompose at 275 and 270 °C, respectively, indicating their high thermal stability.

The colour of the samples changes from green to red during dehydration and this colour change is reversed on exposure to air for one day, suggesting a possible rehydration. To rationalize the observed colour change we performed magnetic susceptibility and spectral measurements of the red complexes. The magnetic study (300 K) revealed the diamagnetic nature of the dehydrated compounds, which is further supported by the solid-state electronic spectra (nujol mull), typical of square-planar Ni^{II} complexes (single peak at $\lambda_{max} \approx 480$ nm). Therefore the dehydration process is definitely accompanied by a structural transformation [octahedral (green) → square planar (red)] around the metal centre. It should be noted that this type of colour change associated with a structural transformation has been reported[10] for several bis-diamine complexes of Ni^{II}, but to the best of our knowledge is uncommon in complexes incorporating tetradentate bis-Schiff base ligands.

Electrosynthesis of $[Ni(L^{1/2})_2]^{3+}$: EPR and Magnetic Evidence

The search for trivalent analogues of **1** and **2** prompted us to carry out electrochemical oxidation (coulometrically) in dry acetonitrile solvent at 1.25 and 1.20 V respectively. The ratio of the observed coulomb count and the calculated coulomb count for the one-electron transfer is very close to unity (0.97 for **1a** and 0.98 for **1b**), suggesting an almost quantitative one-electron oxidation of Ni^{II} precursors to the Ni^{III} derivatives. The cyclic voltammograms of $[Ni(L^{1/2})_2]^{3+}$ (initial scan cathodic) are virtually superimposable with those of $[Ni(L^{1/2})_2]^{2+}$ (initial scan anodic). The observed redox behaviour of the oxidised Ni^{III} species confirms that the coulometric oxidation of $[Ni(L^{1/2})_2]^{2+}$ to $[Ni(L^{1/2})_2]^{3+}$ is accompanied by no major structural change. The uncontrolled decomposition of electrogenerated oxidised species of **2** in solution ruled out any possibility of isolation and further studies. They exist in solution only on the timescale of the voltammetry measurement, thus demonstrating the role of purely kinetic stabilisation[24] in trivalent nickel.

The EPR spectroscopic data of the compounds are listed in Table 4. Polycrystalline samples of **3** at 298 K exhibit an axial spectrum[25] with $g_\perp$ and $g_\parallel$ values of 2.14 and 2.02 respectively (Figure 4). No superhyperfine structure of the $g_\parallel$ component attributed to σ-coupling with the two ^{14}N (imine) atoms coordinated in a mutual *trans* manner is observed. The bond-angle order N^i-Ni-N^i (ca. 179°) > N^p-Ni-N^a (ca. 158°) in the *cis-trans-cis* isomer of $[Ni(L^1)_2]^{2+}$ implies that both steric and electronic requirements will favour the orientation of a linear N^i-Ni-N^i moiety along the *z*-direction. Thus we can reasonably assume that this is also the case for **3** ($3d^7$). The observed *g* inequality ($g_\perp > g_\parallel$) is fully consistent with a tetragonally distorted octahedral geometry with elongation of the axial bond along the *z*-axis.[2,26,27] Hence a strong Jahn−Teller effect must be operative to lift the degeneracy of the e orbital set following the energy order $3d_{x^2-y^2} > 3d_{z^2}$. The spectra of **3** in a frozen (77 K) acetonitrile/toluene (2:1) glass also follow a similar axial pattern as observed for polycrystalline state, strongly indicating that the coordination environment is retained (in solid and solution). The axial spectra at 77 K are important as they suggest that the rhombic field is too weak to split the perpendicular absorption into individual g_{xx} and g_{yy} tensors. The *g* values for these complexes lie well above the spin-only value of a free electron (2.002). This excludes any possibility of the formation of Ni^{II} stabilised ligand radicals. Therefore, the observed EPR signals arise from one metal-centred unpaired electron, in agreement with the trivalent oxidation state.[28]

Table 4. EPR data for trivalent Ni^{III} species.

Compound	$g_\perp$	$g_\parallel$
3a	2.138,[a] 2.137[b]	2.018,[a] 2.018[b]
3b	2.139,[a] 2.139[b]	2.017,[a] 2.018[b]

[a] Polycrystalline state at 298 K. [a] In acetonitrile/toluene (2:1) glass at 77 K.

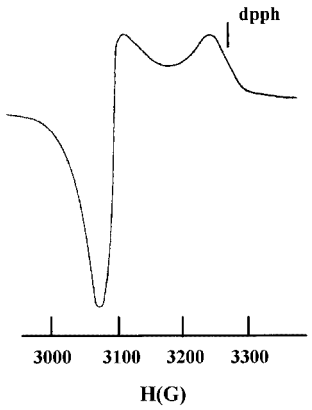

Figure 4. X-band EPR spectrum of $[Ni(L^1)_2]^{3+}$ (**3a**) in the polycrystalline solid state (298 K); instrument settings: power, 30 dB; frequency, 9.1 GHz; modulation, 100 KHz; scan time, 2 min; sweep centre, 3200 G

Further evidence for trivalent nickel complexes is provided by the magnetic moment data. The bulk magnetic moment for **3** at 298 K is consistent with a one-electron paramagnetic behaviour. The effective magnetic moment values of 2.12 and 2.09 μ_B for **3a** and **3b**, respectively, mean that the Ni^{III} complexes are present in a low spin ($t_2^6\ e^1$) configuration with $S = 1/2$. A large orbital contribution to the paramagnetism[24] is noticed, as expected. Unfortunately we were unable to grow single crystals of either **3a** or **3b**, although all the EPR and magnetic data unequivocally suggest the formation of trivalent nickel complexes.

Conclusion

The tridentate and tetradentate ligands presented here are characterised by their different nitrogen donor sites (pyridyl, imine and amino), and their different binding abilities towards a Ni^{II} centre provide us with NiN_6 and NiN_4O_2 types of coordination complexes. Bis-chelates were achieved without deprotonating the amino group. The *cis-trans-cis* isomer of **1** is the only isomer obtained due to steric relaxation, which completely offsets any electronic disadvantage, whereas the *cis-cis-trans* form of **2** is favoured by both steric and electronic factors. The effect of the low π-acidity of the ligands is clearly shown by the predominant localised nature of the bonding in the resulting complexes. Accessible cyclic voltammetric formal potentials of the Ni^{3+}/Ni^{2+} couple for **1** and **2** allowed us to synthesise the related Ni^{III} complexes electrochemically, although the complex formed from **2** is not particularly stable, unlike that formed from **1**.

Proper tuning of the coordination modes of tridentate ligands containing pyridyl, imine and amino donor atoms can afford stable trivalent nickel complexes. The design of such ligands with variable polymethylene spacers and the study of their efficacy to stabilize the higher oxidation states of different metals are in progress.

Experimental Section

Starting Materials: $Ni(ClO_4)_2{\cdot}6H_2O$, 2-acetylpyridine and 2-pyridinecarboxaldehyde were purchased from Aldrich and used as received. HPLC-grade acetonitrile was used for electrochemical, conductivity and UV/Vis work and all other chemicals and solvents were of reagent grade and were used as received.

CAUTION: *Perchlorate salts are hazardous and may explode.*

Physical Measurements: Spectral measurements were carried out using the following equipment: UV/Vis (both in acetonitrile solution and solid), Hitachi U-3501 spectrophotometer fitted with thermostatted cell compartments (sh is shoulder). IR (KBr disc), Perkin−Elmer RXI FT-IR spectrometer and Nicolet Magna IR 750 Series II. A Perkin−Elmer 2400 Series II elemental analyzer was used for microanalysis (C, H, N). EPR spectra was recorded at the X-band on a Varian E-109C spectrometer and calibrated with respect to diphenylpicrylhydrazyl (DPPH, $g = 2.0037$). Solution electrical conductivity was measured in acetonitrile with a Phillips PR 9500 bridge using a platinized electrode; solute concentration was approx. 10^{-3} M. ^1H NMR spectra were recorded on a

Bruker FT 300 MHz spectrometer. The thermal analysis (TG-DTA) was carried out on a Metler Toledo TGA/SDTA 851 thermal analyzer under a dynamic atmosphere of dinitrogen (flow rate: 30 mL·min^{-1}). The sample was heated in an alumina crucible at a rate of 10 °C·min^{-1}. Magnetic susceptibilities were measured on a PAR 155 vibrating-sample magnetometer. Electrochemical measurements were performed under a dinitrogen atmosphere using a PAR model Versastat-2 electrochemical analyzer, with a platinum working electrode. The supporting electrolyte was tetraethylammonium perchlorate (TEAP), and the potentials are referenced to the saturated calomel electrode (SCE) without junction correction.

L^1: Ethylenediamine (0.9 g, 15 mmol) and 2-acetylpyridine (1.815 g, 15 mmol) were mixed in 20 mL of methanol and then refluxed for 3 h. The resulting solution was evaporated to 5 mL and cooled to room temperature. Upon cooling of the solution a yellow solid precipitated. The solid was collected by filtration and was recrystallised from hot methanol affording pale yellow cubes, which were dried in vacuo over fused $CaCl_2$. Yield: 2.11 g (85%). $C_9H_{13}N_3$: calcd. C 66.23, H 8.03, N 25.74; found C 66.17, H 8.07, N 25.81. IR: $\tilde{\nu}$ = 3345−3285 cm^{-1} (ν_{NH_2}), 2950−2850 (ν_{C-H}), 1678 ($\nu_{C=N}$), 1590 (δ_{N-H}), 1447−1302 ($\nu_{pyridine\ ring}$).

L^2: This ligand was prepared by a procedure similar to that for L^1, starting with ethylenediamine (0.9 g, 15 mmol) and 2-pyridinecarboxaldehyde (1.605 g, 15 mmol), to obtain a light-yellow semi-solid which, on recrystallisation from *n*-hexane, gave pale-yellow needles. Yield: 1.84 g (82%). $C_8H_{11}N_3$: calcd. C 64.40, H 7.43, N 28.17; found C 64.32, H 7.37, N 28.23. IR: $\tilde{\nu}$ = 3345−3281 cm^{-1} (ν_{NH_2}), 2952−2847 (ν_{C-H}), 1677 ($\nu_{C=N}$), 1591 (δ_{N-H}), 1450−1302 ($\nu_{pyridine\ ring}$).

L^3: Ethylenediamine (0.9 g, 15 mmol) and 2-acetylpyridine (3.630 g, 30 mmol) were mixed in 25 mL of methanol and then refluxed for 7 h. The resulting solution was evaporated to obtain a yellow semi-solid mass which, on recrystallisation from *n*-hexane, afforded light-yellow needles. The needles were dried in vacuo over fused $CaCl_2$. Yield: 2.44 g (61%). $C_{16}H_{18}N_4$: calcd. C 72.15, H 6.81, N 21.04; found C 72.22, H 6.75, N 21.09. IR: $\tilde{\nu}$ = 2990−2880 cm^{-1} (ν_{C-H}), 1680 ($\nu_{C=N}$), 1450−1307 ($\nu_{pyridine\ ring}$).

L^4: This ligand was prepared by a similar procedure to that employed for L^3, starting with ethylenediamine (0.9 g, 15 mmol) and 2-pyridinecarboxaldehyde (3.210 g, 30 mmol) to give light yellow microcrystals. Yield: 2.29 g (64%). $C_{14}H_{14}N_4$: calcd. C 70.57, H 5.92, N 23.51; found C 70.51, H 5.98, N 23.45. IR: $\tilde{\nu}$ = 2992−2877 cm^{-1} (ν_{C-H}), 1680 ($\nu_{C=N}$), 1451−1306 ($\nu_{pyridine\ ring}$).

$[Ni(L^1)_2](ClO_4)_2$ (1a): $Ni(ClO_4)_2·6H_2O$ (0.165 g, 0.45 mmol) dissolved in the minimum volume of water was added to a solution of L^1 (0.163 g, 0.99 mmol) in methanol (30 mL), and heated to reflux for 2 h to afford a brown solution. The resulting solution was cooled to room temperature and filtered. The filtrate was stripped of solvent under reduced pressure. The residue was washed twice (15 mL each) with hexane to remove the excess ligand and then dried in vacuo over fused $CaCl_2$. Yield: 242 mg (92%). $C_{18}H_{26}Cl_2N_6NiO_8$: calcd. C 37.02, H 4.49, N 14.39; found C 37.09, H 4.45, N 14.46. IR: $\tilde{\nu}$ = 3340, 3290 cm^{-1} (ν_{NH_2}), 2940−2862 (ν_{C-H}), 1658 ($\nu_{C=N}$), 1596 (δ_{N-H}), 1445−1305 ($\nu_{pyridine\ ring}$), 1089, 627 (ν_{ClO_4}).

$[Ni(L^2)_2](ClO_4)_2$ (1b): This complex was prepared by a similar procedure. Yield: 226 mg (90%). $C_{16}H_{22}Cl_2N_6NiO_8$: calcd. C 38.57, H 3.99, N 15.12; found C 38.53, H 4.05, N 15.07. IR: $\tilde{\nu}$ = 3341, 3288 cm^{-1} (ν_{NH_2}), 2942−2862 (ν_{C-H}), 1658 ($\nu_{C=N}$), 1594 (δ_{N-H}), 1441−1307 ($\nu_{pyridine\ ring}$), 1090, 628(ν_{ClO_4}).

$[Ni(L^3)(H_2O)_2](ClO_4)_2$ (2a): $Ni(ClO_4)_2·6H_2O$ (0.304 g, 0.83 mmol) dissolved in 10 mL of water was added to a solution of L^3 (0.266 g, 0.99 mmol) in methanol (40 mL), and heated to reflux for 3 h. The solution turned green. It was then filtered and the filtrate cooled to room temperature. Solvent removal from the filtrate under reduced pressure gave a green residue which was washed twice (10 mL each) with hexane to remove the excess ligand. The compound was then dried in vacuo over fused $CaCl_2$. Yield: 433 mg (93%). $C_{16}H_{22}Cl_2N_4NiO_{10}$: calcd. C 34.32, H 3.96, N 10.01; found C 34.26, H 4.01, N 10.04. IR: $\tilde{\nu}$ =3435−3413 cm^{-1} (ν_{O-H}), 2982−2885 (ν_{C-H}), 1647 ($\nu_{C=N}$), 1603 (δ_{O-H}), 1452−1307 ($\nu_{pyridine\ ring}$), 1096, 626(ν_{ClO_4}), 748 (ρ_r), 609 (ρ_w), 449 (ν_{Ni-O}).

$[Ni(L^4)(H_2O)_2](ClO_4)_2$ (2b): This complex was prepared by a similar procedure. Yield: 407 mg (92%). $C_{14}H_{18}Cl_2N_4NiO_{10}$: calcd. C 31.61, H 3.41, N 10.53; found C 31.55, H 3.48, N 10.50. IR: $\tilde{\nu}$ = 3437−3410 cm^{-1} (ν_{O-H}), 2981−2879 (ν_{C-H}), 1647 ($\nu_{C=N}$), 1604 (δ_{O-H}), 1449−1303 ($\nu_{pyridine\ ring}$), 1095, 625(ν_{ClO_4}), 747 (ρ_r), 610 (ρ_w), 449 (ν_{Ni-O}).

$[Ni(L^1)_2](ClO_4)_3$ (3a): This complex was prepared by an electrochemical technique. The complex $[Ni(L^1)_2](ClO_4)_2$ (0.146 g, 0.25 mmol) was dissolved in dry acetonitrile (30 mL) and TEAP was added as supporting electrolyte. The brown solution was then subjected to coulometric oxidation at 1.25 V vs. SCE under a dinitrogen atmosphere. The solution gradually turned reddish-brown and the oxidation was stopped when the Coulomb count corresponded to a one-electron oxidation. The solvent was then removed under reduced pressure to obtain a reddish-brown solid mixed with TEAP. The residue was dissolved in dichloromethane and TEAP was filtered off. Solvent removal from the filtrate afforded a reddish-brown compound which was then dried in vacuo over fused $CaCl_2$. Yield: 150 mg (88%). $C_{18}H_{26}Cl_3N_6NiO_{12}$: calcd. C 31.63, H 3.83, N 12.30; found C 31.58, H 3.80, N 12.34.

$[Ni(L^2)_2](ClO_4)_3$ (3b): This complex was synthesised by a similar electrochemical procedure in 89% yield. $C_{16}H_{22}Cl_3N_6NiO_{12}$: calcd. C 29.32, H 3.38, N 12.82; found C 29.36, H 3.33, N 12.76.

X-ray Crystallography: Brown or green single crystals of the complexes **1a** and **2a**, respectively, were grown by slow evaporation of solvent from a methanol solution. Data were collected on a Siemens SMART CCD diffractometer with graphite-monochromated Mo-K_α radiation (λ = 0.71073 Å) by the phi and omega scan technique in the range 3° ≤ 2θ ≤ 50° at 293 K. All the data were corrected for Lorentz-polarisation and absorption.[29] The structures were generated by direct methods followed by successive Fourier synthesis and refined by full-matrix least-squares based on F^2. All non-hydrogen atoms were made anisotropic. All the hydrogen atoms (barring water hydrogen atoms) for **2a** were added at the calculated positions. Hydrogen atoms apart from two amino groups (N3, N6) were added at the calculated positions for **1a**. Calculations were performed using the SHELXTAL™ v. 5.03 program package.[30] Significant crystal data are listed in Table 5.
CCDC-216308 (for **1a**) and -216309 (for **2a**) contain the supplementary crystallographic data for this paper. These data can be obtained free of charge at www.ccdc.cam.ac.uk/conts/retrieving.html [or from the Cambridge Crystallographic Data Centre, 12 Union Road, Cam-

Table 5. Crystal data for complexes **1a** and **2a**

Complex	**1a**	**2a**
Formula	$C_{18}H_{26}Cl_2N_6NiO_8$	$C_{16}H_{22}Cl_2N_4NiO_{10}$
M	584.06	559.99
System	monoclinic	orthorhombic
Space group	$P2_1/c$	$P2_12_12_1$
a (Å)	15.5216(13)	11.3061(10)
b (Å)	10.1708(9)	12.9531(12)
c (Å)	15.7458(14)	15.803(2)
α (°)	90	90
β (°)	97.305(2)	90
γ (°)	90	90
V (Å^3)	2465.6(4)	2314.4
Z	4	4
D (mg m^{-3})	1.573	1.607
T (K)	293	293
μ (mm^{-1})	1.059	1.128
Independent reflections	4375	3639
R_{int}	0.0560	0.0347
Collected reflections $[I > 2\sigma(I)]$	10189	7779
$R1$, $wR2$	0.0685, 0.1452	0.0558, 0.1435

bridge CB2 1EZ, UK; Fax: (internat.) +44-1223/336-033; E-mail: deposit@ccdc.cam.ac.uk].

Acknowledgments

One of the authors (S. Banerjee) is thankful to the University Grants Commission (UGC), India, for awarding a Junior Research Fellowship (Sanction no. UGC/548/jr. Fellow Sc.2001/2002).

[1] L. Sacconi, F. Mani, A. Bencini, in *Comprehensive Coordination Chemistry* (Eds.: G. Wilkinson, R. D. Gillard and J. A. McCleverty), Pergamon Press, Oxford, **1987**, vol. 5, ch. 50, pp. 1−347.
[2] K. Nag, A. Chakravorty, *Coord. Chem. Rev.* **1980**, *33*, 87.
[3] L. Gomes, E. Pereira, B. Castro, *J. Chem. Soc., Dalton Trans.* **2000**, 1373.
[4] A. Chakravorty, *Isr. J. Chem.* **1985**, *25*, 99.
[5] [5a] *The Bioinorganic Chemistry of Nickel* (Ed.: J. R. Lancaster, Jr.), VCH, Deerfield Beach, FL, **1988.** [5b]S. M. Hecht, *Acc. Chem. Res.* **1986**, *19*, 383. [5c] Y. Sigura, T. Takita, H. Umezawa,, *Met. Ions Biol. Syst.* **1985**, *19*, 81.
[6] [6a] *Metal-Catalyzed Oxidations of Organic Compounds* (Eds.: R. A. Sheldon and J. K. Kochi), Academic Press: New York, **1981**, 359. [6b] *Catalytic Activation of Dioxygen by Metal Complexes* (Ed.: L. I. Simandi), Kluwer Academic Publishers: Dordrecht, **1992**, 318.
[7] M. T. Maede, D. H. Busch, in *Progress in Inorganic Chemistry* (Ed.: S. J. Lippard), Wiley Interscience: New York, **1985**, 33 and references cited therein.
[8] V. Alexander, *Chem. Rev.* **1995**, *95*, 273 and references cited therein.
[9] J. Lehn, *Pure Appl. Chem.* **1980**, *52*, 2441 and references cited therein.
[10] Y. Ihara, Y. Fukuda, K. Sone, *Inorg. Chem.* **1987**, *26*, 3745 and references cited therein.
[11] S. R. Cooper, *Acc. Chem. Res.* **1988**, *21*, 141.
[12] C. R. Lucas, S. Liu, *J. Chem. Soc., Dalton Trans.* **1994**, 185.
[13] D. Shellmann, H.-P. Neuner, F. Knoch, *Inorg. Chim. Acta* **1991**, *190*, 61.
[14] I. Castro, M. L. Calatayud, J. Sletten, F. Lloret, M. Julve, *J. Chem. Soc., Dalton Trans.* **1997**, 811.
[15] [15a] R. Soules, F. Dahan, J. P. Laurent, P. Castan, *J. Chem. Soc., Dalton Trans.* **1988**, 587. [15b] B. Q. Ma, S. Gao, H. L. Sun, G. X. Xu, *J. Chem. Soc., Dalton Trans.* **2001**, 130.
[16] J. A. C. van Ooijen, J. Reedijk, A. L. Spek, *Inorg. Chem.* **1979**, *18*, 1184.
[17] [17a] E. I. Baucom, R. S. Drago, *J. Am. Chem. Soc.* **1971**, *93*, 6469. [17b] P. Krumholtz, *Struct. Bonding* **1971**, *9*, 139.
[18] [18a] M. A. Robinson, J. D. Curry, D. H. Buch, *Inorg. Chem.* **1963**, *2*, 1178. [18b] H. M. Fischer, R. C. Stoufer, *Inorg. Chem.* **1966**, *5*, 1172.
[19] S. Mukhopadhyay, D. Ray, *J. Chem. Soc., Dalton Trans.* **1995**, 2265.
[20] E. M. Martin, R. D. Bereman, *Inorg. Chim. Acta* **1991**, *188*, 221.
[21] B. J. Henne, D. E. Bartak, *Inorg. Chem.* **1984**, *23*, 369.
[22] I. Nakagawa, T. Shimanouchi, *Spectrochim. Acta* **1964**, *20*, 429.
[23] R. S. Drago, in *Physical Methods in Chemistry*, Saunders: Philadelphia, **1977**, Chapter 11.
[24] L. Fabbrizzi, D. M. Proserpio, *J. Chem. Soc., Dalton Trans.* **1989**, 229.
[25] [25a] G. A. Foulds, *Coord. Chem. Rev.* **1990**, *98*, 1−122. [25b] M. Schroder, *Coord. Chem. Rev.* **1986**, *71*, 139−234.
[26] A. G. Lappin, A. McAuley, *Adv. Inorg. Chem.* **1988**, *32*, 241.
[27] R. I. Haines, A. McAuley, *Coord. Chem. Rev.* **1981**, *39*, 77.
[28] A. Abragam and B. Bleaney, *Electron Paramagnetic Resonance of Transition Metal Ions*, Clarendon, Oxford, UK, **1970**.
[29] G. M. Sheldrick, SADABS, Absorption Correction Program, University of Göttingen, Germany, **1996**.
[30] G. M. Sheldrick, SHELXTL™ v. 5.03, Bruker analytical X-ray systems, Madison, WI, **1994**.

Received November 25, 2003
Early View Article
Published Online April 20, 2004

